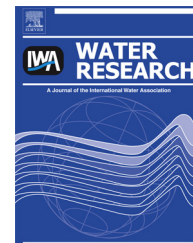




ELSEVIER

Available online at www.sciencedirect.com

ScienceDirect

journal homepage: www.elsevier.com/locate/watres

CrossMark

Bacterially mediated removal of phosphorus and cycling of nitrate and sulfate in the waste stream of a “zero-discharge” recirculating mariculture system

M.D. Krom^{a,b}, A. Ben David^c, E.D. Ingall^d, L.G. Benning^a, S. Clerici^a,
S. Bottrell^a, C. Davies^a, N.J. Potts^a, R.J.G. Mortimer^a, J. van Rijn^{c,*}

^a School of Earth and Environment, Leeds University, UK

^b Charney School of Marine Sciences, Haifa University, Israel

^c The Robert H. Smith Faculty of Agriculture, Food and Environment, The Hebrew University of Jerusalem, Rehovot, Israel

^d School of Earth and Atmospheric Sciences, Georgia Institute of Technology, Atlanta, USA

ARTICLE INFO

Article history:

Received 20 September 2013

Received in revised form

20 February 2014

Accepted 26 February 2014

Available online 11 March 2014

Keywords:

Aquaculture

Anaerobic sludge

Phosphorus removal

Denitrification

Apatite formation

Sulfur cycling

ABSTRACT

Simultaneous removal of nitrogen and phosphorus by microbial biofilters has been used in a variety of water treatment systems including treatment systems in aquaculture. In this study, phosphorus, nitrate and sulfate cycling in the anaerobic loop of a zero-discharge, recirculating mariculture system was investigated using detailed geochemical measurements in the sludge layer of the digestion basin. High concentrations of nitrate and sulfate, circulating in the overlying water (~15 mM), were removed by microbial respiration in the sludge resulting in a sulfide accumulation of up to 3 mM. Modelling of the observed S and O isotopic ratios in the surface sludge suggested that, with time, major respiration processes shifted from heterotrophic nitrate and sulfate reduction to autotrophic nitrate reduction. The much higher inorganic P content of the sludge relative to the fish feces is attributed to conversion of organic P to authigenic apatite. This conclusion is supported by: (a) X-ray diffraction analyses, which pointed to an accumulation of a calcium phosphate mineral phase that was different from P phases found in the feces, (b) the calculation that the pore waters of the sludge were highly oversaturated with respect to hydroxyapatite (saturation index = 4.87) and (c) there was a decrease in phosphate (and in the Ca/Na molar ratio) in the pore waters simultaneous with an increase in ammonia showing there had to be an additional P removal process at the same time as the heterotrophic breakdown of organic matter.

© 2014 Elsevier Ltd. All rights reserved.

* Corresponding author. The Robert H. Smith Faculty of Agriculture, Food and Environment, The Hebrew University of Jerusalem, P.O.Box 12, Rehovot 76100, Israel. Tel.: +972 8 9489302; fax: +972 8 9489024.

E-mail address: jaap.vanrijn@mail.huji.ac.il (J. van Rijn).

<http://dx.doi.org/10.1016/j.watres.2014.02.049>

0043-1354/© 2014 Elsevier Ltd. All rights reserved.

1. Introduction

Fish cages, a widely used industrial mariculture technology, typically discharge up to 80% of the nitrogen and phosphorus that is supplied in the feed into the environment (Naylor et al., 1998; van Rijn, 2013). Land based mariculture offers more control of the waste, but is often limited by the shortage of coastal sites and the cost of inland pumping of seawater and its discharge. The “Zero-Discharge System” (ZDS) is a recently developed sustainable mariculture system (Gelfand et al., 2003) which uses natural microbial processes to control water quality (Cytryn et al., 2003; Gelfand et al., 2003; Neori et al., 2007). The system operates in a completely sealed way, meaning that only a small amount of freshwater is used to replace losses by evaporation. There is no continuous or even intermittent discharge of aqueous effluent to the environment as exists in other mariculture systems. Although the advantages of ZDS mariculture systems in terms of waste output are clear, the mechanisms behind the nitrogen, sulfur and phosphorus cycling in such systems are not well understood.

The ZDS consists of two water treatment loops (Fig. 1). The aerobic loop converts toxic ammonia produced by fish to nitrate by means of a trickling biofilter. In the second loop, an anaerobic loop, consisting of a digestion basin (DB) and fluidized bed reactor, particulate waste organic matter (principally fish feces) and other nutrients are metabolized to environmentally harmless forms. Previous studies on this and similar systems revealed that the major processes affecting the overall water quality are nitrification in the aerobic treatment loop and bacterial breakdown of organic matter by processes including heterotrophic nitrate and sulfate reduction as well as autotrophic nitrate reduction coupled to sulfide oxidation in the DB and fluidized bed reactor (Gelfand et al., 2003; Cytryn et al., 2005; Neori et al., 2007; Sher et al., 2008; Schneider et al., 2011). However the relative contribution of

these anaerobic bacterial processes was not known. Around 70% of the C and N supplied is lost as carbon dioxide and gaseous nitrogen species, presumed to be the result of heterotrophic bacterial respiration (Neori et al., 2007). Of the phosphorus supplied with the fish feed, 21% is taken up for fish growth. Only 5% of the remaining phosphorus accumulates in the water column while the rest is present as solid and pore water phosphorus, mainly in the DB sludge accumulating in the anaerobic treatment loop. It was not known in what form this P accumulates in the sludge nor what processes are controlling this accumulation.

Simultaneous removal of nitrogen (N) and phosphorus (P) by microbial biofilters has been used in a variety of water treatment systems to treat nutrient-rich waste streams. These include systems that use alternating aerobic-anaerobic conditions to trap phosphate as polyphosphate under aerobic (van Loosdrecht et al., 1997) or denitrifying conditions (van Loosdrecht et al., 1998) and release it in a controlled way during the anaerobic cycle. The DB of the ZDS system has free oxygen in the overlying water while the sludge itself is anaerobic with the precise location of the redox boundary depending on the balance of recycling processes within the system. In the DB examined in this study, N and P were found to be simultaneously removed from the waste stream by the accumulation of P in denitrifying organisms under entirely anoxic conditions (Barak and van Rijn, 2000a, 2000b; Barak et al., 2003; Neori et al., 2007).

Similar microbial processes to those in the digestion basin, may occur in natural marine systems particularly in sediments underneath the upwelling regions of the world such as the Benguela current off Namibia and off Oman in the Arabian Sea. These locations have high concentrations of organic matter in the sediment (up to 40%), much of which is labile causing high rates of heterotrophic bacterial activity including sulfate reduction and methane production (Schulz et al., 1999). Phosphorite (diagenetic apatite) nodules often form in

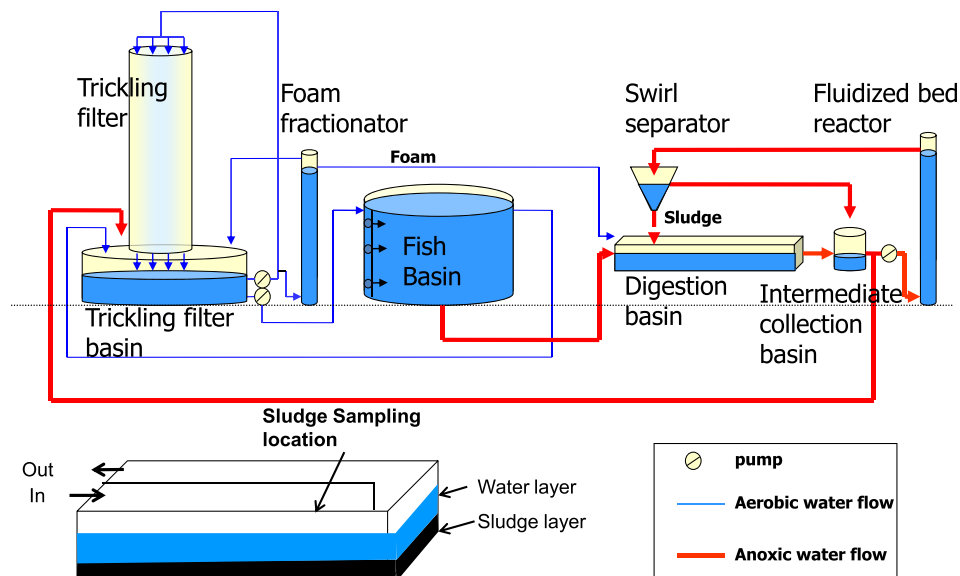


Fig. 1 – A diagram of the system as a whole including a more detailed diagram of the digestion basin showing the location of the sludge sampling.

the sediments beneath these upwelling regions. Two processes have been suggested for this apatite formation. Schenau et al. (2000) suggested that diagenic apatite was formed in pore waters where phosphate released by heterotrophic respiration of organic matter created high enough phosphate concentrations to overcome the kinetic barrier to apatite formation (Van Cappellen and Berner, 1991). More recently, an alternative process has been suggested in which bacteria, particularly sulfide oxidizing bacteria, accumulate polyphosphate, which is then rapidly converted into diagenetic apatite (Goldhammer et al., 2010). Both processes represent a shunt of P from its dissolved form into bacterial biofilms, which is subsequently converted into mineral apatite.

This study examines the types and location of processes that control nitrate, sulfate and phosphorus cycling within the sludge of the anaerobic loop in the ZDS system. The major microbial transformations in the DB were determined using detailed geochemical measurements of the depth distribution of relevant geochemical parameters and their stable isotope composition in the DB sludge layer and the overlying water. Detailed measurements of P in the sludge, pore and overlying waters were made using geochemical and mineralogical methods to determine the P speciation and its changes with depth. The identified P cycling processes are compared and contrasted with similar processes in natural and engineered systems.

2. Material and methods

2.1. System description

The zero discharge system (ZDS) in this study was an enlarged version of the system previously described in detail by Gelfand et al. (2003). Briefly, the system comprised a fish basin (5 m³) stocked with the gilthead seabream (*Sparus aurata*) from which water was circulated through aerobic and anaerobic treatment compartments (Fig. 1). The aerobic compartment consisted of a trickling filter with a volume of 8 m³ and a surface area of 1920 m². Water from the trickling filter was collected in a trickling filter basin (3 m³) which was situated directly underneath the trickling filter. Surface water from the fish basin was circulated through the aerobic compartment at a rate of 10 m³ h⁻¹. The digestion basin (DB, gross volume: 5.4 m³) was the main part of the anaerobic treatment compartment. Water from the bottom of the fish basin was drained continuously (0.8 m³ h⁻¹) into the DB. Effluent water from the DB was recirculated (0.8 m³ h⁻¹) through a fluidized bed reactor (FBR, volume: 13 L) before being returned to the Intermediate Collection Basin. The FBR removes any sulfide or other reduced potentially toxic compounds by microbial oxidation before they reach the fish tank. The DB, with a total surface area of 3.64 m² (2.6 m length; 1.4 m width), contained a partition in the middle of the basin causing the incoming water to flow over a total length of 5.2 m before leaving the basin. Total depth of water and sludge in the DB was 80 cm and sludge thickness ranged between 30 and 50 cm (i.e. the water layer overlying the sludge varied in thickness from 30 to 50 cm). As no

continuous water exchange is required, the system can be operated away from a seawater source. In the absence of such a source and to meet the desired water salinity, solid sea salt was added. During the initial experimental set up, prior to fish being introduced, solid sea salt (Red Sea pHarm Ltd., Israel) was added to the DB. It was allowed to dissolve there and diffuse into the overlying circulating water to a final concentration of ~8500 mgNa/L (i.e. 20 ± 2 ppt). The fish were introduced after the salinity in the recirculating water had reached equilibrium. During the experimental period, local Rehovot tap water was periodically added to the system to compensate for evaporative losses. The system was started in October 2011 with sludge already present from previous operations of the ZDS over the past seven years. This was done to avoid an unacceptably long induction period since we added small fish at first and thus there was limited waste organic matter being supplied to the DB. On October 31, 2010, 738 fish were stocked with an initial weight of 1.5 g and on October 16, 2011, 668 fish were harvested with an average weight of 237.6 g. Feed addition over this period was 241 kg. Hence, the feed conversion coefficient (i.e. total feed addition divided by the total fish weight gained) was 1.53.

2.2. In situ sampling

Water quality parameters sampled in the fish basin were recorded for a period of 360 days starting in October 2011. Oxygen and temperature were measured daily while ammonia, nitrite, nitrate, phosphate, pH and alkalinity were analysed weekly. The sediment system was sampled when anaerobic conditions had been clearly established in the DB sludge (based on removal of nitrate from the overlying water; see Fig S1).

Core samples of sludge from the DB were taken four times from the same location in the digestion basin (see Fig. 1) using a custom-built corer with a rubber diaphragm to seal the bottom. These cores were used for subsequent solid and macropore water analysis. Cores were taken during the morning of July 12th (pore water chemistry and solid analyses), July 13th (for pH) and two cores for isotopic analyses were taken on August 4th (Core A) and February 2nd, 2012 (core B). The first collected core (July 12th, 2011) was taken back to the laboratory and frozen at -20 °C. After 24 h the frozen core was partially thawed (~20 min) and sections of 1 cm each were extruded from the bottom of the core and sliced off with a metal saw. The largest part of the sludge disk was placed in a pre-weighed 50 ml centrifuge tube. It was weighed (wet weight) and then centrifuged for 15 min at 3500 rpm at 4 °C. The supernatant pore waters were filtered through a 0.45 µm filter for phosphate, ammonia and nitrate determination. A subsample was refrozen for subsequent analysis. After thawing, a small known amount of acid was added to the tubes. The acidified samples well mixed, weighed accurately so that the volume of dilution by acid could be determined, and analysed by Inductively Coupled Plasma Atomic Emission Spectroscopy (ICP-AES) for Na, Ca, Mg, P and S. A wet sludge subsample was weighed for porosity determination and then frozen for subsequent freeze-drying. The freeze-dried samples were used for all subsequent solid

samples chemical determinations (see below). A further subsample of each sludge disk was placed immediately into a centrifuge tube containing 5% zinc acetate solution for sulfide determination. In addition, in July, 2011, a sample of fish feces was taken from several fish together with samples of the fish feed for analysis.

The core sampled on July 13th, 2011 for pH measurements was brought back to the lab and sludge samples were siphoned off from the top of the core into a beaker in which pH was measured at the ambient temperature (~ 26 °C). In addition, one sample from the overlying water was taken for pH measurement.

The two cores collected on August 4th, 2011 (Core A) and February 2nd, 2012 (Core B) were immediately frozen after sampling and transported to Leeds with dry ice. In Leeds, the cores were extruded frozen, cut into the required depth intervals for analysis, and trimmed. The ice formed from overlying water at the top of each core was melted for analysis and sulfate recovery. Each sample was split into two and each refrozen. One aliquot was weighed, dried at 110 °C and reweighed to determine water content. The other aliquot was placed frozen into a sealed extraction cell and flushed with N_2 . Pore-water components were extracted by diffusional exchange (Bottrell et al., 2000; Spence et al., 2005) for chemical analysis and recovery of sulfate as $BaSO_4$. Freezing of core may cause redistribution of solutes during freezing; however the effects are minimized since the cores are subsampled at a coarse resolution and completely thawed to extract solutes. Freezing prevents both post-sampling oxidation of S species and physical disturbance/mixing of the core during transport, each of which would introduce far greater artefacts.

2.3. Pore water and solid sludge determinations

Pore water samples were determined for major cations and anions by ICP-AES and ion chromatography. Samples used for analysis of cations were acidified with two drops of HCl (37%). Deionized water was added to some of the samples to facilitate the dissolution of any observed precipitate. Elemental concentrations were measured using a Side-On-Plasma ICP-AES model 'ARCOS' (Spectro GmbH, Germany). Samples for determination of nitrate, sulfate, chloride, and phosphate were forced through Reverse Phase filters and through 0.25 μm membrane filters to remove organic material. The above anions were determined using an ICS-3000 Ion Chromatograph (Dionex Corporation, Sunnyvale, California), with an AS17 analytical column, an AG17 guard column, and an ASRS-Ultra II Anion Micromembrane Suppressor. Total ammonia (NH_3 , NH_4^+), from here on referred to as ammonia, was determined with the salicylate-hypochlorite method as described by Bower and Holm-Hansen (1980). Dissolved sulfide was analysed on samples fixed with ZnAc with the methylene blue method of Cline (1969).

Freeze dried sludge samples, feed and fish feces were analysed for P speciation using the procedure of Aspila et al. (1976) to determine total P and inorganic P (and hence by difference: organic P). In addition, adsorbed P was determined using the first step of the SEDEX P speciation procedure of Ruttenberg (1992) involving extraction by $MgCl_2$. Extracted samples were

determined for phosphate using the molybdate blue reaction (Golterman et al., 1978). The standard error (1s) of these analyses was adsorbed P 3% ($n = 12$), inorganic P 8% ($n = 16$) and organic P 4% ($n = 16$). An additional solid subsample of sludge was analysed for major elements on fused glass beads prepared from ignited powders using a sample to flux ratio of 1:10 (Lithium tetraborate) on PANalytical XRF spectrometer at University of Leicester, UK. Quantification of inorganic polyphosphate was accomplished using a fluorometric technique based on the interaction of inorganic polyphosphate with 4',6'-Diamidino-2-phenylindole (DAPI) (Aschar-Sobbi et al., 2008; Diaz and Ingall, 2010). DAPI is commonly used as a stain for nucleic acid but will also bind to polyphosphate, which is then detected using a combination of incident and observed wavelengths optimized for polyphosphate (Aschar-Sobbi et al., 2008). Inorganic polyphosphate of at least 15 P atoms in size is quantified independently of chain length to a detection limit of 0.5 μM (Diaz and Ingall, 2010). Typical errors associated with this technique are $\pm 15\%$ (Diaz and Ingall, 2010).

For the isotope cores, after pore-water extraction, acid-volatile (AVS = dissolved sulfides and solid monosulfides) and chromium reducible sulfur (CRS = pyrite sulfur and elemental sulfur) were extracted from the solid phase and recovered as a single CuS precipitate for isotopic analysis. The mass of S recovered was determined titrimetrically (Newton et al., 1995). Residual sulfur in the solid phase is presumed to be organic-bound S and was converted to $BaSO_4$ by Eschka fusion and determined gravimetrically. In addition, the 'Red Sea salt' and Rehovot tap water used to create half seawater conditions in the system were sampled. The Red Sea salt was dissolved for chemical analysis and sulfate recovered as $BaSO_4$ for both S and O isotopic analysis.

The oxygen isotopic composition of aqueous sulfate was determined on $BaSO_4$ precipitates using the method described by McCarthy et al. (1998) and using a VG SIRA 10 gas source isotope ratio mass spectrometer. Data are reported as $\delta^{18}O$ in per mille (‰) relative to the Vienna Standard Mean Ocean Water (V-SMOW); reproducibility (2 x standard error), estimated from replicate analyses of standards, is 0.3‰ or better. Sulfur extracts and fish feed samples were quantitatively converted to SO_2 by combustion at 1150 °C in the presence of pure oxygen (N5.0) injected into a stream of helium (CP grade). The combustion gases were quantitatively converted to N_2 , CO_2 and SO_2 by passing them through tungstic oxide. Excess oxygen was removed by reaction with hot copper wires at 850 °C and water was removed in a magnesium perchlorate or Sicapent trap. All solid reagents were sourced from Elemental Microanalysis, UK, and all gases were sourced from BOC, UK. N_2 continued through the system unchecked, whilst CO_2 and SO_2 were removed from, and re-injected into, the gas stream using temperature controlled adsorption/desorption columns. The $\delta^{34}S$ was derived using the integrated mass 64 and 66 signals relative to those in a pulse of SO_2 reference gas (N3.0). These ratios are calibrated to the international V-CDT scale using an internal laboratory barium sulfate standard derived from seawater (SWS-3), which has been analysed against the international standards NBS-127 (+20.3‰), NBS-123 (+17.01‰), IAEA S-1 (−0.30‰) and IAEA S-3 (−32.06‰) and assigned a value of +20.3‰, and an inter-lab chalcopyrite standard CP-1 assigned a value of −4.56‰. If samples were

more ^{34}S depleted than CP-1, the IAEA S-3 standard was used instead. The precision obtained for repeat analyses of standard materials was generally better than 0.3‰ $\delta^{34}\text{S}_{\text{REF}}$ (1 standard deviation).

3. Results

3.1. Water analyses

The water quality was determined weekly in the circulating water of the ZDS system (Fig. S1). The detailed sampling took place on July 12th, when main water quality parameters had stabilized and ammonia, phosphate, nitrate and nitrite values were 0.02 mM, 1.03 mM, 16.1 mM and 0.017 mM, respectively. The nitrate concentration in the overlying water at the time of sampling (17.4 mM) was much higher than in the surface sludge. There was a decrease in nitrate such that the nitrate concentration below 20 cm was close to or below the practical limit of detection. The nitrate decrease within the sludge can be explained by the fact that under anoxic conditions nitrate is reduced by bacteria, which oxidise organic matter and other reduced compounds.

Sulfate is also respired under anoxic conditions within the sludge. In order to recognize biologically mediated changes in sulfate in the sludge, it was necessary to compare its concentration to that of sodium since the former compound is found in measurable amounts in the sea salt added to the system. There was a systematic increase in Na observed with depth with values increasing from $\sim 50\%$ seawater concentration at the surface to 4 times higher concentration at the base of the sludge core (Fig. S2A). This increase was most probably caused by the specific manner in which sea salt was added to the system prior to the experimental period. Salt was added to the DB with a working volume of 2.9 m^3 (approximately 25% of the total water volume in the system). Although intended to completely dissolve in the total system water, it appears that as a result of this mode of salt addition, relatively more salt accumulated in the bottom layers of the DB. Despite the high porosity of the sludge (0.95 in the top layers and decreasing to 0.85 at 35 cm depth), there was no evidence of physical mixing (Fig. S2C). Sulfate decreased rapidly from a value of 60.1 (SO_4 mM/Na M) in the overlying water to 14.8 (SO_4 mM/Na M) at 2.5 cm depth (Fig. 2A). The ratio continued to decrease with depth to a minimum value of 4.3 (SO_4 mM/Na M) at 14.5 cm and then increased to 43.9 (SO_4 mM/Na M) at the lowest point sampled (33.5 cm). A similar profile was obtained when (total dissolved sulfur minus dissolved sulfide)/Na was plotted with depth (Fig. 2A). There was no measurable sulfide in the overlying water; it increased to a maximum of 3.8 mM at 15.5 cm and then decreased to a value of 1.1 mM at 34.5 cm (Fig. 2B).

In order to understand the diagenetic processes in the sludge, the concentration of relevant chemical species and parameters were measured. Phosphate and ammonia are commonly measured as the products of the heterotrophic anaerobic respiration of organic matter. However, the concentration of these chemical species depends on the sum of all diagenetic processes in the sludge. Thus, the dissolved phosphate in the sludge depth profile (Fig. 3A) was lower in the

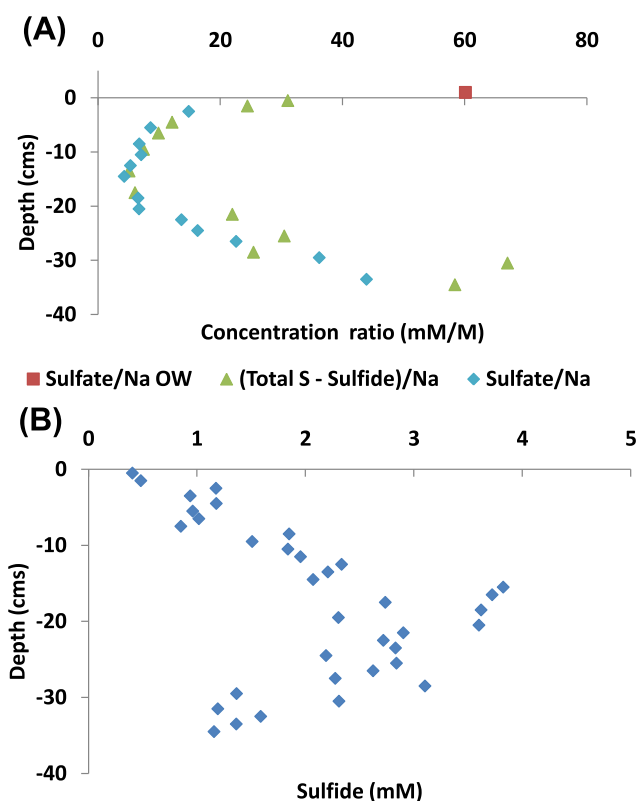


Fig. 2 – Pore water concentration of A) Sulfate/Na and {Total dissolved S (measured by ICP) minus dissolved Sulfide)/Na concentration ratio (mmolesS/moleNa) and B) Dissolved Sulfide (molesS/l) in the pore waters of the sludge. Measured value for sulfate/Na molar ratio in the overlying water (OW) is given. There was no sulfide detected in the overlying water.

uppermost layers (1.12 mM) compared with the overlying water (1.4 mM) and decreased with depth to values of ~ 0.7 mM at 35 cm. By contrast, ammonia (Fig. 3B) was much higher in the surface sludge compared with the overlying water. The ammonia concentrations in the upper 20 cm were roughly constant in the range of 13–15 mM, which then decreased to ~ 10 mM below 25 cm.

Further information about the nature of the diagenetic processes in the sediment comes from measurements of pH. In the sludge, the pH increased from 6.35 in the overlying water to a maximum of 6.8 just below the sediment water interface (SWI) and then decreased with depth to a value of 6.5 at the base of the sludge (Fig. S2D).

The concentration ratios of Ca/Na and Mg/Na were determined to provide information about the possible precipitation of inorganic P minerals in the sludge. The molar ratio in the overlying waters (21.96) was within error the same molar ratio of Ca/Na (mM/M) in normal seawater (Fig. S2B). The ratio increased just below the sludge–water interface to 40.7 and then decreased with depth reaching values of ~ 5 at 35 cm. The Mg/Na (mM/M) remained essentially constant at 60–78 over the depth profile analysed (not shown).

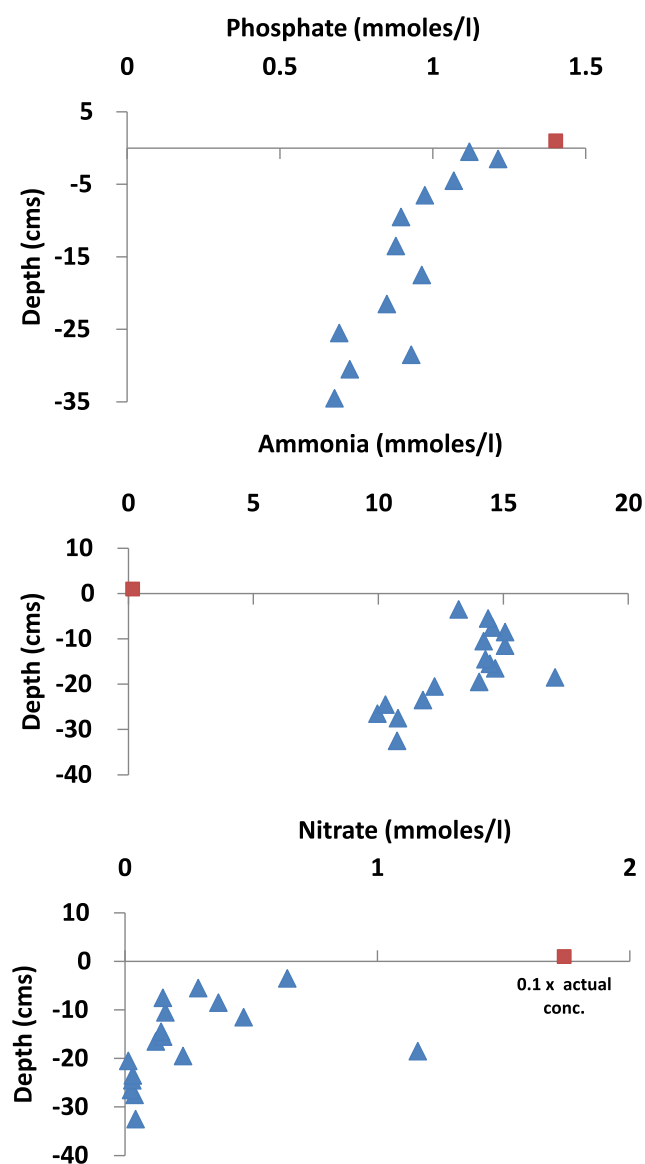


Fig. 3 – Pore water nutrient concentrations of dissolved phosphate, ammonia and nitrate vs depth together with corresponding values for these nutrients in the overlying water. Note that the concentration of nitrate in the overlying water is 17.4 mM as noted in the data point description.

3.2. Solid sludge phase

The P speciation and content of the sludge was compared with feces (the major input) and fish feed (a possible minor input) to characterise the transformations which have occurred in the DB. The total P in the sludge varies from ~1500 $\mu\text{molesP/g}$ in the surface layers increasing to a maximum of 2090 $\mu\text{molesP/g}$ at 15.5 cm and decreasing to 1100 $\mu\text{molesP/g}$ at the base of the sludge (Fig. 4A). Inorganic P was the major phase in the sludge and increased from surface values of 1030 $\mu\text{molesP/g}$ to >1500 $\mu\text{mol/g}$ before decreasing to 1120 $\mu\text{mol/g}$ at 35.5 cm. By contrast, organic P was relatively constant over the upper 20 cm at ~400–500 $\mu\text{molesP/g}$ and then decreased to

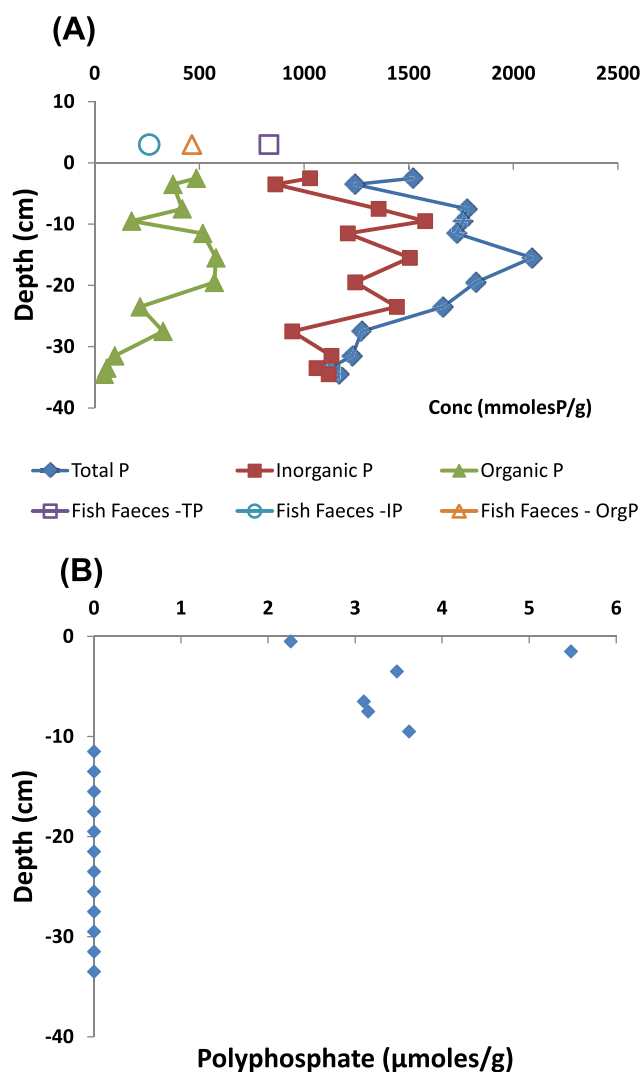


Fig. 4 – Phosphate in sludge: (A) Changes in P speciation with depth in sludge of the sedimentation basin together with the P speciation of the fish feces which is the main input of particulate matter to the digestion basin; (B) Polyphosphate concentrations ($\mu\text{mole/g}$) with depth.

<50 $\mu\text{mol/g}$ at the base of the sludge (Fig. 4A). The total P content of the fish feed (410 $\mu\text{molesP/g}$) was lower than the fish feces (830 $\mu\text{molesP/g}$), which is the main source of particulate matter to the sludge. In contrast to the sludge, the organic P content of the fish feces (465 $\mu\text{molesP/g}$) was higher than its inorganic P content (260 $\mu\text{molesP/g}$; Fig. 4a; Table S1). The principal major element in the sludge was Ca, which increased from 2.3 mmolesCa/g (9.3 wt%Ca) at the surface to 3.2–4.1 mmolesCa/g (12.8–16.4 wt%Ca) at depth (Table S2). Other elements, which might bind with P (Fe and Al), were present only in $\mu\text{moles/g}$ concentrations (Table S2).

3.2.1. Sulfur mass balance

Sulfur mass balance can be assessed in the cores used for S isotopic determinations as concentrations were also measured (Table 1). Data are presented as aqueous concentrations for dissolved species and corrected to concentrations

Table 1 – Sulfur species concentrations in sludge cores (average of two cores). NB: centred values are aqueous concentrations, right adjusted values in bold are recalculated to total sludge volume, taking account of porosity changes.

Depth range cm	Dissolved phase					Solid phase		
	Sulfate		Sulfide		Total S	Organic S	CRS	Total S
	mM	mmol/L sludge	mM	mmol/L sludge	mmol/L sludge	mmol/L sludge	mmol/L sludge	mmol/L sludge
Overlying water	14.2	14.2	0	0	14.2	0	0	0
0 to 2.5	7.8	7.4	0.4	0.4	7.8	128	453	581
2.5 to 5	7.0	6.6	1.1	1.0	7.6	51	539	589
5 to 10	5.9	5.5	1.4	1.3	6.8	90	506	597
10 to 15	4.2	3.8	2.1	1.9	5.7	210	720	930
15 to 19	2.5	2.2	3.5	3.1	5.3	112	855	968
19 to 23	0.7	0.6	2.9	2.6	3.4	228	862	1091
23 to 26	1.4	1.2	2.7	2.3	3.5	378	1271	1649
26 to 29	2.5	2.1	2.7	2.3	4.4	410	967	1377
29 to 32	4.8	4.1	1.5	1.3	5.4	377	815	1191

in total sludge for all species (assuming a linear transition between measured porosities of 0.95 at core top and 0.85 at core base). As noted above, sulfate concentrations decline with depth in the upper part of the core (14.2 mM in the overlying water, 7.8 mM in the uppermost core, declining to a minimum of 0.7 mM at ~20 cm depth). However, although sulfide concentrations increase over a similar interval (0 mM in the overlying water, 0.4 mM in the uppermost core, reaching a maximum of 3.5 mM at ~17 cm depth) they never match the losses in sulfate and thus total dissolved S decreases with depth over this interval. This imbalance is explained by the general increase in concentration of solid phase S species over the same depth interval (from ~590 mmol S/L of sludge in the upper core to >1000 mmol S/L of sludge in the deepest core; Table 1), as sulfide reacts with solid phase components to produce new organic S and CRS species. Elemental S may be a product of sulfide reoxidation (e.g. Jiang et al., 2009) and this is analysed within the CRS fraction.

3.3. Stable isotope ratios

3.3.1. Inputs to the system

The 'Red Sea salt' used to make up the tank water contained sulfate with isotopic compositions of $\delta^{34}\text{S} = -1.5\text{‰}$ and $\delta^{18}\text{O} = 10.0\text{‰}$ (Fig. 5); this is not a typical marine sulfate isotope composition as the sulfate is sourced from terrestrial sulfate deposits. The local Rehovot tap water used to fill the tank contains 0.16 mM sulfate with isotopic composition of $\delta^{34}\text{S} = 6.9\text{‰}$ and $\delta^{18}\text{O} = 7.8\text{‰}$. As the circulating tank water was made up to 50% seawater chloride concentration, the dissolved sulfate was dominated by the added Red Sea salt. Fresh water resources (both groundwater and river waters) in Israel typically have a narrow range of $\delta^{18}\text{O}$ between -4‰ and -6‰ (Gat and Dansgaard, 1972) and the tap water used should be in this range. The other main source of S to the system was the fish food, which contains ~0.7 wt% S; two different batches of food were analysed and had slightly different $\delta^{34}\text{S}$ isotopic compositions, 6.5‰ and 8.9‰ (Fig. 5).

3.3.2. Solid phase sulfur isotopic composition

The combined acid-volatile (AVS) and chromium reducible sulfur (CRS) content of the sludge was similar in both cores

and showed no systematic variation with depth, ranging from 3.45 to 10.5 mg g⁻¹. Organic-S contents were lower (0.81–3.54 mg g⁻¹) and again showed no strong depth trend (Table S3). Both forms of S in the sludge show a similar and quite narrow range of S isotopic composition (AVS + CRS = 1.4‰–8.2‰; Org-S = 3.6‰–8.3‰, Fig. 5, Table S3) and no systematic variation with depth. The S isotopic composition of pore-water sulfate was broadly similar in both cores, particularly so in the upper part of each core (Fig. 5). The lowest $\delta^{34}\text{S}$ value occurred in the shallowest pore-water sample and was lighter than the sulfate in the overlying water (7.3‰ vs. 8.8‰ in core A and 8.0‰ vs. 10.2‰ in core B, differences of 1.5‰ and 2.2‰). Below this, sulfate $\delta^{34}\text{S}$ remained near constant with depth down to 17 cm and had values closely similar to the sulfate in the overlying water. Below 17 cm depth the two profiles diverged somewhat, though in general there was a tendency to higher $\delta^{34}\text{S}$ in the lower part of the profiles. Sulfate $\delta^{18}\text{O}$ in the shallowest pore-waters was lower than in the overlying water but initially increased with depth in both profiles. In the deeper pore-waters there is more variability in sulfate $\delta^{18}\text{O}$ and Core A tended to more elevated values (>+10‰) while core B tended to lighter values (~+2‰); it should be noted that SO₄/Cl was different for the two cores in their deeper parts.

3.3.3. Calculation of the amount of total P in the sludge and the fraction accumulated during the present phase of pond operation

The total sludge volume was calculated to be 960,000 cm³ based on a tank surface area of 2.4 m² and a depth of sludge of 40 cm. With an average sludge porosity of 0.9, it could be calculated that the DB contained 96,000 cm³ of sediment particles. Assuming a dry density of 1.4 g/cm³, this equals 134,400 g of sediment. Using 1535 mmol P/g as the average total P content of the sediment, it is calculated that the sludge contains 206 mol P. Our calculation of the total P supplied to the ZDS as fish feed minus the fish growth during the present run (October 2010 until July 2011) was 65 mol P. This figure assumes that the only location for P accumulation is the DB and that there was no major residual P build up in the nitrifying filter or elsewhere. As a result, this is a minimum estimate. Since P in the sludge cannot go anywhere, this implies

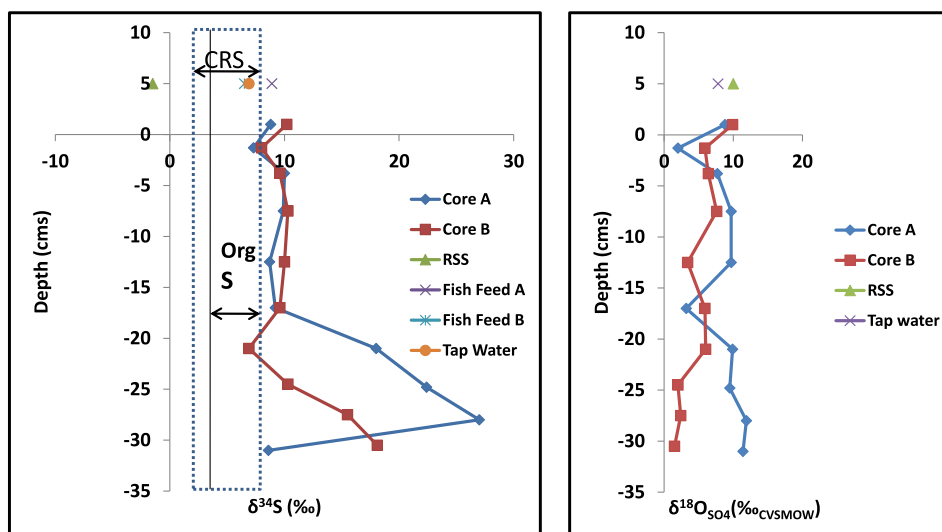


Fig. 5 – Depth profiles of $\delta^{34}\text{S}$ and $\delta^{18}\text{O}$ of dissolved sulfate for two sludge cores with depth. Also shown are $\delta^{34}\text{S}$ and $\delta^{18}\text{O}$ of sulfate in the overlying waters and values for input sources (Red Sea Salt (RSS) and tap water). On the left hand diagram the ranges depicted in boxes are for solid phase S species in the core; CRS = chromium reducible sulfur (monosulfides + pyrite + elemental S), Org S = organic sulfur; $\delta^{34}\text{S}$ values are also plotted for fish feed.

that there were 141 mol of P already in the sludge before the system was started. The system had been operating for seven years intermittently before the start of this run. Therefore we conclude that the sludge before we started in October, 2010 was already a long term repository of P, built up during previous cycles of the ZDS system operating in a similar way to the present run.

3.3.4. Phosphate minerals within the sludge

The X-ray diffraction data of the freeze-dried but untreated core section and fish feces samples revealed a high background signal (due to high organic matter concentrations) with main peaks identifiable as calcite, fluorapatite and gypsum. The fish feed sample contained the same phases but with higher proportions of apatite and with additional calcium oxalates and hydroxyapatite (Fig. S3A). After the ashing and washing all carbon phases (organic matter and calcite) as well as the highly soluble gypsum were, as expected, absent from the scans (Fig. S3B). It is worth noting that with XRD it was difficult to differentiate between the various, crystalline forms of apatite (A) in these samples. However, a clear distinction between less crystalline hydroxyapatite (HAP) and other Ca–P phases was observable but not quantifiable due to the broadness of the peaks. Looking at the XRD scans of the treated samples compared with the fish feces, which is the main source of organic matter in the sludge, a clear difference can be seen in the nature of the Ca–P phases present (Fig. S3B). There was a shift in the peak position for the apatite phases (labelled A) to a lower angle and a decrease in peak height. The less crystalline HAP peak also shifted to lower angles but increased in peak height and a new peak, possibly assignable to Francolite (a carbonate rich form of fluor-apatite), appeared in the sludge. Within the upper 13.5 cm of the sludge, the peaks for all Ca–P phases remained relatively constant in both angle and relative magnitude. Between 19.5 cm and 34.5 cm

(data not shown) the peak locations remained constant though the relative peak heights decreased somewhat. In none of the scans were there any peaks that could be assigned to struvite.

4. Discussion

4.1. P and N dynamics

High concentrations of nitrate in the water flowing over the DB sludge on July 12th (17.4 mM) compared to much lower concentration of nitrate just below the SWI (0.6 mM; Fig. 3C) are consistent with intense microbial denitrification in the DB. In addition to rapid and extensive denitrification, heterotrophic sulfate reduction caused ~75% of the sulfate present in the overlying water to be reduced within the upper 2.5 cm of the sludge. This sulfate reduction resulted in an accumulation of free sulfide in the pore waters up to a maximum of 3.8 mM at ~15 cm. Despite the build up of free sulfide in surface layers of the sludge, no free sulfide was measured in the fish tank or circulating water. Previous studies have shown that this was due to autotrophic denitrification (especially in the fluidized bed reactor) and other sulfide oxidation processes efficiently removing any sulfide, which might leak from the sludge (Cytryn et al., 2005; Neori et al., 2007; Sher et al., 2008; Schwermer et al., 2010; Neori and Mendola, 2012).

In this study, we have used measurements of stable isotopes of S and O ($\delta^{34}\text{S}$ and $\delta^{18}\text{O}$) in the solids and pore waters of the sludge tank to examine the nature of the microbial processes in the DB. Water sampled from the system (overlying water and pore water) contains sulfate that has significantly higher $\delta^{34}\text{S}$ than the sulfate initially added to the system (i.e. ~10‰ vs. -1.4‰). This results from a combination of two effects: (1) during the operation of the system, fish feed with a

more elevated $\delta^{34}\text{S}$ has been constantly added and processing of this sulfur may have added sulfate with higher $\delta^{34}\text{S}$ to the sulfate pool and (2) at the present time, S accumulating in the solid phase (both as AVS + CRS and Org-S) has lower $\delta^{34}\text{S}$ than the sulfate in the system (Fig. 5). If this solid phase pool has gradually accumulated S with lower $\delta^{34}\text{S}$ than the contemporaneous sulfate, then this will have driven the aqueous sulfate to progressively higher $\delta^{34}\text{S}$.

The $\delta^{34}\text{S}$ of pore-water sulfate in the upper 17 cm varies little from that of the overlying water. However, the chemical data for pore-waters show large decreases in SO_4/Cl in the upper parts of both cores, which would normally imply removal of sulfate by microbial sulfate reduction. This process is usually accompanied by a large sulfur isotope fractionation (e.g. Canfield, 2001) with sulfide produced typically 20‰–45‰ depleted in ^{34}S compared to sulfate. However, in this particular reactor this process seems to operate with much smaller fractionation. Firstly, there is only a small offset between pore-water sulfate compositions and average solid phase sulfide, with only ~5‰ depletion in ^{34}S in the sulfide product and secondly there is no large systematic increase in sulfate $\delta^{34}\text{S}$ as SO_4/Cl falls in the upper parts of both cores (data not shown but similar to the SO_4/Na profile (Fig. 2A)). However, the sulfate in the pore-water is not inert, as there are large changes in sulfate $\delta^{18}\text{O}$ over this interval in both profiles (Fig. 5). Rather, sulfide produced must be near-quantitatively reoxidized to sulfate and there is little net conversion of sulfate to reduced forms such as AVS, CRS or Org-S (e.g. Bottrell et al., 2009). However, as sulfate is reduced and reoxidized the re-formed sulfate contains oxygen atoms from different sources and with different $\delta^{18}\text{O}$ to the original sulfate. The fact that sulfate in the shallowest pore-water has slightly lower $\delta^{34}\text{S}$ than the overlying water or deeper pore-water indicates that production of sulfate by reoxidation of ^{34}S -depleted sulfide dominates at this level. The $\delta^{18}\text{O}$ of this sulfate is lower than the overlying waters (by 6.8‰ in Core A and 4.0‰ in Core B, Fig. 5). Such a shift to lower $\delta^{18}\text{O}$ in sulfate rules out molecular oxygen as the oxidizing agent as it is highly ^{18}O enriched, but rather indicates that the oxygen atoms incorporated into sulfate during sulfide oxidation are derived from water molecules with negative $\delta^{18}\text{O}$ (McCarthy et al., 1998; Bottrell and Tranter, 2002; Bottrell et al., 2009) and thus sulfide oxidation was driven by an alternative electron acceptor, most likely nitrate, based on the chemical profiles (Fig. 3C). Thus, it is concluded that in the upper layers of the DB there is rapid heterotrophic sulfate reduction, which is approximately balanced by autotrophic nitrate reduction.

Heterotrophic nitrate reduction is a relatively lesser process. To test the feasibility of such a scenario the system was investigated using a simple model of the fate of S and N species.

The model considers the budgets of sulfur and nitrogen species in a system where heterotrophic sulfate reduction (HSR), heterotrophic nitrate reduction (HNR) and autotrophic nitrate reduction (ANR, using sulfide as an electron donor) may occur. Starting compositions were those of the overlying water (15 mM sulfate, 15 mM nitrate and zero sulfide); reactions were modelled as first-order with respect to these components. Concentration of organic substrate for heterotrophic respiration was not considered to limit those reactions. The model describes the evolution of an aliquot of pore-water as its composition is modified by these reactions. Model runs were performed with different ratios of reaction rates, i.e. $R_{\text{HSR}}/R_{\text{HNR}}$ and $R_{\text{ANR}}/R_{\text{HNR}}$. Because sulfate is a lower energy-yielding electron acceptor, under similar conditions R_{HSR} is generally lower than R_{HNR} , so all runs were made with $R_{\text{HSR}}/R_{\text{HNR}} \leq 1$. Experimental determination of the effect of sulfide on nitrate reducing systems shows that $R_{\text{ANR}} > R_{\text{HNR}}$, with autotrophic activity often effectively eliminating heterotrophic activity as long as sulfide is present (e.g. Sher et al., 2008; Shijie et al., 2010), so all model runs were made with $R_{\text{ANR}}/R_{\text{HNR}} \geq 1$.

Model results are presented in Table 2. During most runs initially heterotrophic NR dominated, but as sulfide concentration increased due to SR, rates of autotrophic NR increased and became dominant (except in runs with very low heterotrophic SR/heterotrophic NR where nitrate was consumed before autotrophic NR became dominant). Where the rate of autotrophic NR is much greater than that of heterotrophic NR, little nitrate is consumed by heterotrophic NR before autotrophic NR becomes dominant and sulfide concentrations are low (and sulfate concentrations remain high) until all nitrate is consumed. Thus, under many realistic scenarios the system evolves such that SR is the dominant heterotrophic respiration mechanism and the sulfide generated then accounts for the majority of NR via an autotrophic pathway. This pattern is consistent with the observed chemistry and stable isotope compositions that show that sulfate is cycled but not consumed in the sludge over the interval where nitrate is consumed. Also shown in Table 2 are the sulfide concentrations at which autotrophic NR becomes dominant; these are lower than the observed concentrations in the sludge profile, indicating that ample sulfide is available to drive autotrophic NR. Sulfide concentrations rise in the model runs after nitrate

Table 2 – Output data for model runs. The two values in each grid square give: (1) % of nitrate consumed by heterotrophic nitrate reduction before consumption by autotrophic nitrate reduction becomes dominant (* indicates runs where all nitrate was consumed before autotrophic NR became dominant); (2) concentration of sulfide at which autotrophic nitrate reduction becomes dominant (or final sulfide concentration for runs marked*).

Heterotrophic SR rate/Heterotrophic NR rate	Autotrophic NR rate/heterotrophic NR rate		
	1	10	100
1	8.8%; 1.01 mM	1.1%; 0.15 mM	0.4%; 0.15 mM
0.33	40.8%; 1.01 mM	26.7%; 0.15 mM	1.2%; 0.05 mM
0.1	73.1%; 1.01 mM	63.3%; 0.11 mM	4.1%; 0.015 mM
0.03	89.3%; 0.69 mM*	86.0%; 0.38 mM*	52.7%; 0.005 mM*

concentrations fall, conditions similar to those observed deeper in the sludge profile.

4.2. Sediment sludge as a long term sink for P

The digestion basin is a bacterial bioreactor in which the sediment sludge is predominantly a repository of organic rich fish feces from the fish basin. Inputs to the DB are modified subsequently mainly by anaerobic bacterial processes with the major bacterial transformations described above. Despite the high fraction of organic P in the fish feces input most of the particulate P in the DB is not organic P but inorganic P (Fig. 4A, Table S1). X-Ray diffraction data indicates that the P accumulating in the DB is a mixture of crystalline apatite and poorly ordered hydroxyapatite (Fig. S3). There was no evidence of struvite. The XRD data, however, showed that the fish feed contained large amounts of crystalline apatite and some hydroxyapatite (probably as ground up fish bone from the fishmeal; Fig. S3A) besides oxalates and calcite. Part of this initial apatite probably survives through the gut of the *S. aurata* and is excreted within the fish feces (Fig. S3B, top XRD scan). We ask the question whether the apatite measured in the sludge is simply the residue of accumulating apatite supplied externally alone or whether it is also formed actively in the sludge by *in situ* processes. The sludge in the uppermost layer represents most closely the (transformed) fresh organic matter input from the fish tank. We assume initially that the particulate matter reaching the sludge surface was 100% fish feces because of good evidence for this based on observations and on the observed fish growth, i.e. that the fish ate essentially all the food they were fed. The total P measured in the surface sludge was 1520 $\mu\text{molesP/g}$, which is higher in total concentration than either the fish feces (830 $\mu\text{mol/g}$) or the fish feed (410 $\mu\text{mol/g}$; Table S1). It is known that there is significant denitrification and loss of C by CO_2 and/or methane production in the ZDS system. Neori et al. (2007) estimated that over a period of 500 days approximately 70% by weight was lost from the system as gaseous nitrogen and carbon dioxide. The calculated loss of weight in the conversion of 832 $\mu\text{molesP/g}$ to 1520 $\mu\text{molesP/g}$ is 46% assuming that the total P remained constant. This change in concentration for a period of 220 days was reasonable based on the results of Neori et al. (2007) for a similar ZDS system. If we assume that all of the change in measured inorganic P was only due to this loss of total mass then the inorganic phase should be 480 $\mu\text{molesP/g}$ compared with the measured inorganic P (1035 $\mu\text{molesP/g}$) and the organic P was calculated to be 850 $\mu\text{molesP/g}$ compared with the measured 480 $\mu\text{molesP/g}$ of organic P. Thus, in addition to any changes in concentration caused by loss of mass, there also had to be a major and rapid conversion of organic P to inorganic P.

The sludge tank is a location of active heterotrophic nitrate and sulfate reduction. There was major accumulation of ammonia and phosphate in the pore waters (Fig. 3), an increase in pH (Fig. S2D) as well as rapid reduction in nitrate and sulfate, which are all characteristic of heterotrophic bacterial reduction. However in the upper 10 cm, which is the zone of most active heterotrophic reduction, while ammonia increased with depth by ~ 2 mM, phosphate decreased by ~ 0.2 mM. This requires a process within the upper layers of

the sludge, which caused a net removal of phosphate while ammonia (and presumably phosphate) was being released by heterotrophic reduction. Phosphate could be removed by the formation of polyphosphate granules in denitrifying and other reducing bacteria. However while polyphosphate was present in the upper 10 cm, it was only found in $\mu\text{moles/g}$ amounts (Fig. 4B) which was not sufficient to explain this major removal of phosphate unless this represented a transient phase. A more likely explanation is the formation of mineral apatite. Struvite, another possible mineral that could be removed in such systems, would require the removal of both ammonia and phosphate simultaneously. Our high-resolution X-Ray diffraction scans over the 50–55° 2θ range (which is a location where apatite can clearly be separated from hydroxyapatite and other Ca–P phases) showed the presence of hydroxyapatite peaks in both the fish feces and the sludge. However, as described above, there was a clear change in the nature and proportions of the crystalline and poorly ordered Ca–P phases with depth (Fig. S3B) indicating that new, secondary Ca–P phases – most likely additional hydroxyapatite and maybe francolite have formed. It needs to be noted that the input of crystalline apatite from the fish feces and possibly also the fish feed makes a quantitative determination of these changes difficult.

Using our measured pore water concentrations, the degree of saturation of the pore waters for possible insoluble chemical species was carried out using PHREEQC thermodynamic software in the upper layers of the sediment sludge. In addition to measured pore water species (Fig. 3), we assumed a fluoride concentration of half that in normal seawater (based on the Na and Cl concentrations which are similar conservative elements and are measured as half seawater concentration). The bicarbonate concentration was obtained from DIC measurements on gel probes corrected for incomplete back equilibration assuming that Cl and bicarbonate were equally affected. The calculation showed that the pore waters were supersaturated with respect to hydroxyapatite, aragonite, calcite and dolomite but not with respect to anhydrite, gypsum or struvite (Table 3).

Over the same depth interval (0–17 cm) as phosphate decreases by 0.2 mM (Fig. 3), dissolved Ca decreases by 6 mM and the Ca/Na ratio decreased from 40 to ~ 10 (Fig. S2B) while solid phase Ca increased from 2.33 mmolCa/g to 4.24 mmolCa/g (Table S2) and inorganic carbonate-C increased by a factor of 2 (Fig. S2E). This means that $\sim 15\%$ of the Ca in the sludge is CaCO_3 (assuming that all inorganic C is CaCO_3) and the remainder is apatite. Taken together, these data suggest that these upper layers of the sludge are the site of active precipitation of both hydroxyapatite and calcite from the pore waters of the sludge. The precipitation of hydroxyapatite is facilitated in this system because not only were the pore waters highly supersaturated with respect to apatite but also there were available apatite nuclei in the shape of the ground up fish bones added via the fish food. Attempts to observe directly the nature of the apatite formation process using XANES measurements using synchrotron were not successful mainly because there were simply too many phosphorus-rich granules in the observed field to observe the necessary subtle changes in peak shapes predicted.

Table 3 – Calculated degree of saturation of the major minerals most likely to be formed by diagenetic processes in the sedimentation basin sludge. The calculations were carried out using PHREEQC thermodynamic software and the pore water data measured in this study (see text). Note that minerals with a positive Saturation Index (SI) are oversaturated and potentially able to precipitate depending on the kinetics of precipitation. IAP is the Ion Activity Product and can be used to calculate the solubility constant (log KT) by the relationship $\log KT = \log (IAP) - SI$.

Phase	Saturation index (SI)	Log IAP	Log KT	Mineral formula
Anhydrite	–1.16	–5.52	–4.36	CaSO ₄
Aragonite	1.74	–6.60	–8.34	CaCO ₃
Calcite	1.88	–6.60	–8.48	CaCO ₃
Dolomite	4.15	–12.94	–17.09	CaMg(CO ₃) ₂
Gypsum	–0.96	–5.44	–4.58	CaSO ₄ · 2H ₂ O
Hydroxyapatite	6.86	3.44	–3.42	Ca ₅ (PO ₄) ₃ OH
Struvite	–1.94	2.72	–13.5	Mg(NH ₄)(PO ₄) · H ₂ O

Our data also shows that in the longer term there was a conversion of organic P to apatite within the digestion basin. At the time of the start up of this particular ZDS run, there was sludge in the DB, which was the residue from seven years of pond operation in various different modes i.e. different masses and sizes of fish but fundamentally still being operated as a ZDS system. This residual sludge was expected to contain the end products of ZDS processes. The observed depth profile of the sludge showed an increase in inorganic P (i.e. apatite P) with depth and a synchronous decrease in the proportion of organic P within the system particularly in the lower layers (>25 cm) where the almost all of the organic P appears to have converted in a process analogous to the sink switching observed in recent marine sediments (Ruttenberg and Berner, 1993) into inorganic apatite.

4.3. Synthesis comparing processes in DB to other systems

The ZDS was designed to use natural bacterial processes found in marine systems, particularly in marine sediments, to control water quality conditions over long periods of time (several months to years). These processes, which include nitrification, oxic respiration, heterotrophic nitrate and sulfate reduction and autotrophic nitrate reduction by sulphide, are balanced in such a way as to keep the water quality conditions in the fishpond within levels acceptable for fish growth. Our results here suggest that the closest natural analogue for P cycling processes in the DB are the sediments beneath modern upwelling regions such as off Namibia and in the Arabian Sea (e.g. Goldhammer et al., 2011; Schenau et al., 2000). These are sediments with very high levels of organic matter (up to 40% OM). They are locations with intense rates of heterotrophic bacterial respiration including both oxic processes and sulfate reduction. The sediments underneath upwelling currents are the major areas for phosphorite (apatite) formation. Schenau et al. (2000) observed high rates of authigenic apatite formation, which they suggest, are induced by high rates of organic matter degradation producing phosphate in the pore waters. They also suggest that dissolution of fish debris acts as an additional source of dissolved phosphate. The high concentration of dissolved phosphate together with normal levels of calcium in the pore waters result in sufficient over saturation with respect to apatite (francolite) precipitation to overcome the kinetic barrier known to exist in less

organic rich ‘normal’ marine sediments (Van Cappellen and Berner, 1991).

An alternative mechanism for apatite precipitation has been suggested by Goldhammer et al. (2010, 2011) who suggest that polyphosphate present in sulfide oxidizing bacteria is rapidly converted to apatite. This process occurs under anoxic conditions and they calculate that the rate of phosphate to apatite conversion by this process exceeds the rate of phosphorus release during organic matter mineralisation. It is possible that both of these processes are occurring in the DB since there is direct evidence of both heterotrophic breakdown of organic matter and extensive oxidation of sulfide and the presence of polyphosphate in the uppermost active layers of the DB. It is however not possible with the data collected in this study to determine which of these processes dominate in the formation of apatite.

The phosphate that is removed from the recirculating system and accumulates in the DB is mineral apatite. Apatite is the form of phosphate, which is most commonly used as the primary mineral for commercial phosphate applications. In a world with dwindling exploitable reserves of phosphorite and other phosphate minerals it is important to recycle phosphorus. Since apatite is acid soluble, the conversion of solid apatite from the sludge into dissolved P would be relatively easy. Thus the P accumulated in this system could be easily recovered and converted into a form of phosphorus that could be used in such applications as fertilizers.

5. Conclusions

The following conclusions can be derived from the results presented in this study:

- The digestion basin of a zero-discharge recirculating mariculture system is a major sink of phosphorus as well as the main site for the removal of nitrogen as a result of the conversion of nitrate to gaseous nitrogen by denitrification initially heterotrophic but eventually mainly autotrophic.
- Inorganic sulfur in the digestion basin is rapidly recycled through heterotrophic sulfate reduction and autotrophic sulfide oxidation.
- In the upper sludge layers of the digestion basin with ample levels of labile carbon, dissolved sulfate and nitrate,

bacterial heterotrophic respiration is dominated by sulfate reducers providing sulfide for subsequent use in the process of autotrophic denitrification.

- Under anoxic, nitrate and sulfate-rich conditions, inorganic phosphate is removed from the pore waters in the sludge layers through apatite formation. Authigenic apatite is precipitated from the pore waters, which are supersaturated with respect to hydroxyapatite. Two possible pathways are suggested for this authigenic apatite formation: (1) precipitation of apatite from phosphate released by heterotrophic respiration of organic matter containing P combining with Ca from seawater in the presence of apatite nuclei added via the fish food or (2) nucleation of apatite involving bacterial polyphosphate as a transient but crucial phase. Our data were not able to differentiate between these two possible pathways.

Acknowledgements

We would like to thank David Ashley for his help and advice with many aspects of the chemical analyses carried out in this project and in particular for the inspirational way in which he carried out sampling and analysis late into the night during the major sampling trip in Israel. We also thank Amir Neori for his useful comments on the text. This work was funded by a UK–Israel BIRAX grant (BY2/BIO/01) to JvR and MDK and by a USA–Israel Binational Science Foundation grant (2008216) to JvR and EI. LGB would also like to acknowledge part support for her work during this project through a UK Natural Environment Research Council award (NE/C004566/1).

Appendix A. Supplementary data

Supplementary data related to this article can be found at <http://dx.doi.org/10.1016/j.watres.2014.02.049>.

REFERENCES

- Aschar-Sobbi, R., Abramov, A.Y., Diao, C., Kargacin, M.E., Kargacin, G.J., French, R.J., Pavlov, E., 2008. High sensitivity, quantitative measurements of polyphosphate using a new DAPI-based approach. *J. Fluoresc.* 18, 859–866. <http://dx.doi.org/10.1007/s10895-008-0315-4>.
- Aspila, K.I., Aqemian, H., Chau, A.S.Y., 1976. A semi-automated method for the determination of inorganic, organic and total phosphate in sediments. *Analyst* 101, 187–197.
- Barak, Y., van Rijn, J., 2000a. Biological phosphorus removal in a prototype recirculating aquaculture system. *Aquac. Eng.* 22, 121–136.
- Barak, Y., van Rijn, J., 2000b. Atypical polyphosphate accumulation by the denitrifying bacterium *Paracoccus denitrificans*. *Appl. Environ. Microbiol.* 66, 1209–1212.
- Barak, Y., Cytryn, E., Gelfand, I., Krom, M., van Rijn, J., 2003. Phosphate removal in a marine prototype recirculating aquaculture system. *Aquaculture* 220, 313–326.
- Bottrell, S.H., Tranter, M., 2002. Sulphide oxidation under partially anoxic conditions at the bed of the Haut Glacier d'Arolla, Switzerland. *Hydrol. Process.* 16, 2363–2368.
- Bottrell, S.H., Parkes, R.J., Cragg, B.A., Raiswell, R., 2000. Isotopic evidence for deep anoxic pyrite oxidation and stimulation of bacterial sulphate reduction. *J. Geol. Soc.* 157, 711–714.
- Bottrell, S.H., Mortimer, R.J.G., Davies, I.M., Harvey, S.M., Krom, M.D., 2009. Sulphur cycling in organic-rich marine sediments from a Scottish fjord. *Sedimentology* 56, 1159–1173.
- Bower, C., Holm-Hansen, T., 1980. A salicylate-hypochlorite method for determining ammonia in seawater. *Can. J. Fish. Aq. Sci.* 37, 794–798.
- Canfield, D.E., 2001. Isotope fractionation by natural populations of sulfate-reducing bacteria. *Geochim. Cosmochim. Acta* 65, 1117–1124.
- Cline, J.D., 1969. Spectrophotometric determination of hydrogen sulfide in natural waters. *Limnol. Oceanogr.* 14 (3), 454–458.
- Cytryn, E., Barak, Y., Gelfand, I., van Rijn, J., Minz, D., 2003. Diversity of microbial communities correlated to physiochemical parameters in a digestion basin of a zero-discharge mariculture system. *Environ. Microbiol.* 5, 55–63.
- Cytryn, E., van Rijn, J., Schramm, A., Gieseke, A., de Beer, D., Minz, D., 2005. Identification of bacterial communities potentially responsible for oxic and anoxic sulfide oxidation in biofilters of a recirculating mariculture system. *Appl. Environ. Microbiol.* 71, 6134–6141.
- Diaz, J., Ingall, E.D., 2010. Fluorometric quantification of natural inorganic polyphosphate. *Environ. Sci. Technol.* 44, 4665–4671. <http://dx.doi.org/10.1021/es100191h>.
- Gat, J.R., Dansgaard, W., 1972. Stable isotope survey of the fresh water occurrences in Israel and the northern Jordan rift valley. *J. Hydrol.* 16, 177–212.
- Gelfand, I., Barak, Y., Even-Chen, Z., Cytryn, E., Krom, M., Neori, A., van Rijn, J., 2003. A novel zero-discharge intensive seawater recirculating system for culture of marine fish. *J. World Aquac. Soc.* 34, 344–358.
- Goldhammer, T., Bruchert, V., Ferdelman, T.G., Zabel, M., 2010. Microbial sequestration of phosphorus in anoxic upwelling sediments. *Nat. Geosci.* 3 (8), 557–561.
- Goldhammer, T., Brunner, B., Bernaconi, S.M., 2011. Phosphate oxygen isotopes: Insights into sedimentary phosphorus cycling from the Benguela upwelling system. *Geochim. Cosmochim. Acta* 75 (13), 3741–3756.
- Golterman, H.L., Clymo, R.S., Ohnstad, M.A.M., 1978. Methods for Physical and Chemical Analyses of Freshwaters, second ed. In: *International Biological Programme Handbooks*; no. 8. Blackwell Scientific Publ, Oxford, U.K, p. 210.
- Jiang, G., Sharma, K.R., Guissola, A., Keller, J., Yuan, Z., 2009. Sulfur transformation in rising main sewers receiving nitrate dosage. *Water Res.* 43, 4430–4440.
- McCarthy, M.D.B., Newton, R.J., Bottrell, S.H., 1998. Oxygen isotopic compositions of sulphate from coals: implications for primary sulphate sources and secondary weathering processes. *Fuel* 77, 677–682.
- Naylor, R.L., Goldberg, R.J., Mooney, H., Beveridge, M.C., Clay, J., Folk, C., Kautsky, N., Lubchenco, J., Primavera, J., Williams, M., 1998. Nature's subsidies to shrimp and salmon farming. *Nature* 282, 883–884.
- Neori, A., Krom, M.D., van Rijn, J., 2007. Biochemical processes in intensive zero-effluent marine fish culture with recirculating aerobic and anaerobic biofilters. *J. Exp. Mar. Biol. Ecol.* 349, 235–247.
- Neori, A., Mendola, D., 2012. An anaerobic slurry module for solids digestion and denitrification in recirculating, minimal discharge marine fish culture systems. *J. World Aquac. Soc.* 43, 859–868.
- Newton, R.J., Bottrell, S.H., Dean, S.P., Hatfield, D., Raiswell, R., 1995. An evaluation of the chromous chloride reduction

- method for isotopic analyses of pyrite in rocks and sediment. *Chem. Geol.* 125, 317–320.
- Ruttenberg, K.C., 1992. Development of a sequential extraction method for different forms of phosphorus in marine sediments. *Limnol. Oceanogr.* 37, 1460–1482.
- Ruttenberg, K.C., Berner, R.A., 1993. Authigenic apatite formation and burial in sediments from non-upwelling, continental margin environments. *Geochim. Cosmochim. Acta* 57, 991–1007.
- Schenau, S., Slomp, C.P., DeLange, G.J., 2000. Phosphogenesis and active phosphorite formation in sediments from the Arabian Sea oxygen minimum zone. *Mar. Geol.* 169 (1–2), 1–20.
- Schneider, K., Sher, Y., Erez, J., van Rijn, J., 2011. Carbon cycling in a zero-discharge mariculture system. *Water Res.* 45 (7), 2375–2382.
- Shijie, A., Tang, K., Nemati, M., 2010. Simultaneous biodesulphurization and denitrification using an oil reservoir microbial culture: effects of sulphide loading rate and sulphide to nitrate loading ratio. *Water Res.* 44, 1531–1541.
- Sher, Y., Schneider, K., Schwermer, C.U., van Rijn, J., 2008. Sulfide induced nitrate reduction in the sludge of an anaerobic treatment stage of a zero-discharge recirculating mariculture system. *Water Res.* 42, 4386–4392.
- Schulz, H.N., Brinkhoff, T., Ferdelman, T.G., Marine, M.H., Teske, A., Jorgensen, B.B., 1999. Dense populations of a giant sulfur bacterium in Namibian shelf sediments. *Science* 284, 493–495.
- Spence, M.J., Thornton, S.F., Bottrell, S.H., Spence, K.H., 2005. Determination of interstitial water chemistry and porosity in consolidated aquifer materials by diffusion equilibrium-exchange. *Environ. Sci. Technol.* 39, 1158–1166.
- Schwermer, C.U., Ferdelman, T.G., Stief, P., Gieseke, A., Rezakhani, N., van Rijn, J., de Beer, D., Schramm, A., 2010. Effect of nitrate on sulfur transformations in sulfidogenic sludge of a marine aquaculture biofilter. *FEMS Microbiol. Ecol.* 72, 476–484.
- Van Cappellen, P., Berner, R.A., 1991. Fluorapatite crystal growth from modified seawater solutions. *Geochim. Cosmochim. Acta* 55, 1219–1234.
- van Loosdrecht, M.C.M., Brandse, F.A.M., de Vries, A.C., 1998. Upgrading of wastewater treatment processes for integrated nutrient removal – the BCFS process. *Water Sci. Technol.* 37, 209–217.
- van Loosdrecht, M.C.M., Hooijmans, C.M., Brdjanovitch, D., Heijnen, J.J., 1997. Biological phosphate removal processes. *Appl. Microbiol. Biotechnol.* 48, 289–296.
- van Rijn, J., 2013. Waste treatment in recirculating aquaculture systems. *Aquac. Eng.* 53, 49–56.